miR-124 Contributes to the Functional Maturity of Microglia

Adam J. Svahn,[1]* Jean Giacomotto,[1]* Manuel B. Graeber,[1,2] Silke Rinkwitz,[1,3] Thomas S. Becker[1,3]

[1] Brain and Mind Research Institute, Sydney Medical School, University of Sydney, Sydney, Australia

[2] Faculty of Health Sciences, University of Sydney, Sydney, Australia

[3] Department of Physiology and School of Medicine, University of Sydney, Sydney, Australia

ABSTRACT: During early development of the central nervous system (CNS), a subset of yolk-sac derived myeloid cells populate the brain and provide the seed for the microglial cell population, which will self-renew throughout life. As development progresses, individual microglial cells transition from a phagocytic amoeboid state through a transitional morphing phase into the sessile, ramified, and normally nonphagocytic microglia observed in the adult CNS under healthy conditions. The molecular drivers of this tissue-specific maturation profile are not known. However, a survey of tissue resident macrophages identified *miR-124* to be expressed in microglia. In this study, we used transgenic zebrafish to overexpress *miR-124* in the *mpeg1* expressing yolk-sac-derived myeloid cells that seed the microglia. In addition, a systemic sponge designed to neutralize the effects of *miR-124* was used to assess microglial development in a *miR-124* loss-of-function environment. Following the induction of *miR-124* overexpression, microglial motility and phagocytosis of apoptotic cells were significantly reduced. *miR-124* overexpression in microglia resulted in the accumulation of residual apoptotic cell bodies in the optic tectum, which could not be achieved by *miR-124* overexpression in differentiated neurons. Conversely, expression of the *miR-124* sponge caused an increase in the motility of microglia and transiently rescued motility and phagocytosis functions when activated simultaneously with *miR-124* overexpression. This study provides *in vivo* evidence that *miR-124* activity has a key role in the development of functionally mature microglia. © 2015 Wiley Periodicals, Inc. Develop Neurobiol 00: 000–000, 2015

Keywords: microglia; miRNA; development; phagocytosis; chemotaxis

INTRODUCTION

The development of yolk-sac derived primitive myeloid cells precedes the onset of hematopoietic monocyte differentiation and a subset of the former migrate to become the self-sustaining microglial population (Ginhoux et al., 2010; Kierdorf et al., 2013; Hoeffel et al., 2015). In zebrafish, the first stages of transition from yolk-sac derived primitive macrophages toward the mature microglial phenotype involve repeated conversions ("morphing") between amoeboid motile microglia and highly branched sessile microglia (Svahn et al., 2013). The molecular

definition of these different forms of microglia and how they are controlled genetically are outstanding questions.

MicroRNAs (miRNAs) are ~22nt small-RNA molecules that act as well-conserved post-transcriptional regulators (Bartel, 2009). miRNAs regulate a multitude of pathways as evidenced by conserved miRNA binding sequences in a large proportion (>60%) of mammalian mRNAs (Friedman et al., 2009). *miR-124* is highly expressed in the nervous system, constituting 25%–48% of CNS miRNAs (Lagos-Quintana et al., 2002) and has been identified in a wide range of invertebrates (Isik et al., 2010) and vertebrates (Lim et al., 2003), including mammals (Lagos-Quintana et al., 2002).

In the neuronal lineage, *miR-124* is a suppressor of antineural identity signaling that helps drive neural progenitors toward a stable neuronal fate (Makeyev et al., 2007; Visvanathan et al., 2007). Shortly after a neural stem cell (NSC) commences commitment toward the neural progenitor pathway, *miR-124* expression is induced and is necessary for the transition to a rapidly proliferating progenitor cell (Åkerblom et al., 2012). Once NSCs are committed to the neuronal lineage, *miR-124* continues to suppress the progenitor identity factors laminin-γ and integrinβ1 (Cao et al., 2007) to promote neurite outgrowth (Yu et al., 2008) and to support maturation and survival as in the case of dentate gyrus granule neurons and retinal cones by suppressing Lhx2 (Sanuki et al., 2011).

In the myeloid lineage, *miR-124* expression is now recognized as a transcriptomic marker that distinguishes microglia from systemic macrophages in homeostasis. Expression of *miR-124* has been identified in F4/80^{+}, CD11b^{+} CNS resident microglia and when expressed in bone marrow derived macrophages mediates downregulation of pathological response markers (MHCII, CD45, CD86, F4/80, CD11b, TNFα, iNOS) via binding to a target site in transcription factor C/EBPα mRNA and in turn downregulating PU.1 (Spi1) (Ponomarev et al., 2011). Further, preclinical administration of *miR-124* has been found to alter the progression of experimental autoimmune encephalomyelitis (EAE), significantly ameliorating the pathological response of the microglia, preventing leukocyte infiltration, mitigating inflammatory lesions, and preventing the onset of disease symptoms.

The stimulation of normal resident ramified microglia to become full-blown macrophages in a graded manner (functional plasticity of microglia) is typically associated with pathology and can result in impaired functioning of the CNS (Graeber, 2010).

During zebrafish development, microglia undergo a transition from an early highly motile amoeboid form with phagocytic functions to a sessile, exquisitely branched state (Svahn et al., 2013). To investigate *miR-124* as a possible mechanism involved in this microglial transition, we used transgenic overexpression of *miR-124* and expression of an mRNA decoy (Ebert et al., 2007; Ebert and Sharp, 2010), or sponge, that neutralizes *miR-124* activity to investigate the influence of *miR-124* on microglial behavior during early CNS development.

MATERIALS AND METHODS

Zebrafish Care

Zebrafish (*Danio rerio*) were maintained under standard conditions (Westerfield, 2000). Experimental protocols were approved by the University of Sydney Animal Ethics Committee. Transgenic lines were generated by injection of Tol2 flanked constructs and transposase. Larvae were raised in E3 medium at 28°C on a 14:10 light:dark cycle. The age of the larvae used in the study precludes sex determination.

mir-124 and *miR-218* Overexpression Constructs

Synthetic *dre-pri-miR124-1* was amplified from Zebrafish DNA (primers: forward, 5′- CTGCTTCGAGAGAGA GATTCAAGTC-3′; reverse: 5′-GTCCAATCAACGGT-TAACTTCA-3′). PCR product was introduced in pDONR221 gateway compatible clone via BP clonase reaction. Synthetic *dre-pri-miR124-1* was then inserted in 107-UAS-YFPs-Gtwy-clmc2CHERRY via LR clonase reaction. 107-UAS-YFPs-Gtwy-cmlc2CHERRY is a modified version of pBH-UAS-YFP-Gtwy from Michael L. Nonet's laboratory, in which the YFP's stop codon was restored.

107-UAS-YFPs-miR124-cmlc2CHERRY was injected in one-cell stage wild type embryos. Embryos were sorted based on mCherry expression in the heart, and 50 animals were raised to adult stage. F[0] founders were identified via outcross with wild type, based on fluorescent expression in the heart of resulting embryos.

hsa-miR-218-2 was isolated from human DNA and developed into a transgenic line by the above method (primers: forward, 5′-CAAAGGATGC AGATACAGAGGG-3′; Reverse, 5′-CGTCAGAGAGAG GACAGGAG-3′).

Anti-*miR124* Sponge (SP124) Construct

To express the sponge on a ubiquitous promotor, βactin:mCherry:10xSP124 was generated. We performed a LR reaction with the following multisite-gateway-compatible clones: 299 (p5E-bactin), 386 (pME-mCherry), homemade p3E-10xSP124 and destination clone 394

pDestTol2pA2. Homemade p3E-10xSP124 contains 10x anti-*miR124* sponge sequences that were synthesized by Biobasic (https://store.biobasic.com/gene-synthesis/).

*β*actin:mCherry:10xSP124 was injected into one-cell stage wild type zebrafish embryos. Fifty animals expressing mCherry were sorted and raised to adult stage. Adults were outcrossed with wild type to identify F[0] founders that produced embryos with strong red fluorescent expression, indicating a strong expression of anti-*miR124* sponges.

Imaging

Larvae were embedded in 1% low melting point agarose as detailed in Svahn et al. (2013). Confocal imaging was carried out on a Zeiss LSM 710. Lasers used were 488 nm and 561 nm. The objectives used were Zeiss W Plan-Apochromat 20x and 40x water immersion objectives. Time lapses were captured in 7.5 minute intervals over a 3-hour period.

Image Analysis

Processing of images was conducted in ImageJ. Cell motility was carried out by tracking with the Manual Tracker plugin (created by F. Cordelières, http://rsbweb.nih.gov/ij/plugins/track/track.html). Phagocytic profile was obtained by visually inspecting the time lapse for each cell included and identifying the number of instances of phagocytosis. Uncontacted apoptotic cell identification was carried out by marking a $50 \times 50 \times 50 \ \mu m^3$ cube in the optic tectal region of the brightfield stack channel and counting opaque, irregularly shaped cells within the region. In previous work, there was a 1:1 correlation between these cells in brightfield and AnnexinV bound apoptotic cells. Cells currently inside microglial cells or with a microglial process physically opposed were considered to have entered the phagocytosis pathway.

Blinded Development and Survival Assay

At 24 hpf larvae were visually inspected, and two groups of 25 larvae from each transgene were distributed into coded petridishes (transgene name obscured) and raised as normal in E3 medium. Larvae were fed paramecia from 5 days post fertilization (dpf) as standard. An experimenter not involved in the collection or coding of the larvae then conducted visual inspections at 2, 3, 4, 5 and 13dpf as well as touch response testing at 3 and 4dpf. A successful touch response consisted of a motor response during a maximum of five light touches with a 0.16 mm syringe tip on the anterior dorsal portion of the head.

Statistical Analysis

Analysis was conducted in R. Bootstrap; resampling consisted of 10,000 resamples. 95% confidence intervals and *p*-values are reported (Altman and Bland, 2011).

RESULTS

Transgenic *miR-124* Overexpression and Knockdown by a *miR-124* Sponge

To overexpress *miR-124* in macrophages and microglia, we used a construct containing the *dre-pri-miR-124-1* sequence (miRBase accession: MI0001966) of zebrafish under the control of the *mpeg1* promoter (Ellett et al., 2011; Svahn et al., 2013). Figure 1(A) illustrates the structure of pre-*miR-124* and the alignment of Zebrafish pre-*miR-124* copies 1-6 with mouse and human pre-*miR-124* copies 1-3, showing the high level of conservation for this pre-miRNA.

A *miR-124* sponge was constructed using an mRNA sequence containing a repeated *miR-124* target sequence (SP124, see methods). As illustrated in Figure 1(B), the sponge was designed with a short mismatch, or "bulged" sequence, that prevents complete binding, thus increasing stability and efficiency; incomplete binding weakly induces the mRNA breakdown cascade and further reduces the activity of the *miR-124*-RISC complex (Ebert et al., 2007; Otaegi et al., 2012). *miR-124* is a highly expressed neuronal miRNA, and microglia may take up exogenous miRNA as a consequence of phagocytosis and pinocytosis (Chen et al., 2015) or exosome transfer (Valadi et al., 2007; Lachenal et al., 2011; Chen et al., 2012). Therefore, a ubiquitous promoter (*β*actin) was chosen for sponge expression in this study. On this background, a direct *mpeg1* promoter driving eGFP expression was used to visualize microglia.

Represented in Figure 1(C), *dre-pri-miR-124-1* and YFP were driven by a UAS promoter which is activated by the Gal4 transcription factor in the Gal4-UAS transgenic system (Scott, 2009). The sponge construct consisted of an mCherry sequence followed by a 10x repeat of the *miR124* sponge driven by a *β*actin promoter. Transgenic larvae carrying the UAS:YFP-*dre-pri-miR-124-1* construct were crossed into an *mpeg1*:Gal4 transgenic line driving expression in macrophages and microglia. A control in which *miR-124* was expressed in postmitotic neurons was generated by crossing an *elavl3*-driven Gal4 activator line (HuC:Gal4) (Paquet et al., 2009) with the UAS:YFP-*dre-miR-124-1* overexpression line. A further control in which *miR-218* was overexpressed in place of *miR-124* was generated as above with a UAS driven *hsa-miR-218-2* (miRBase accession: MI0000295).

To validate the activity and specificity of the sponge for *miR-124* and the successful processing and activity of the artificial *miR-124*, we coinjected

Figure 1 *miR-124* structure and transgene architecture. A: Alignments (ClustalW) of the pri-*miR-124* from zebrafish, mouse, and human. The coloured regions in pink and blue represent the left and right arms of the pre-miRNA, with the yellow representing the hairpin region. B: The sponge sequence (upper strand) binding domain of the mature *miRNA-124* sequence (lower strand). C: The architecture of the overexpression (upper) and sponge (lower) transgenes. The overexpression transgene contains the UAS promoter driving the YFP sequence and the *dre-miR-124-1* sequence in the forward direction and a *cmlc2* promoter driving mCherry expression in the reverse direction. The sponge transgene contains a ubiquitous promoter (*β*actin) promoter driving mCherry and a 10x repeat of the above sponge sequence in the forward direction. D: Validation of synthetic *miR124* and anti-*miR124* sponge (SP124) transgenic expression/activity. Transgenic animals *β*actin:mCherry:SP124, which ubiquitously express mCherry protein fused to 10x SP124 repeats (Fig. 1B,1C), were injected with two plasmids simultaneously (i) 503UNC:Gal4 that expresses Gal4 specifically in muscle cells and (ii) UAS:YFP-*miR124* that expresses YFP fluorescent protein fused to synthetic *miR124* (Fig. 1C). Muscle-specific expression of synthetic *miR124* induced by 503UNC:Gal4 can be tracked by the presence of YFP (processed in green in the present pictures), and correlated with downregulation of mCherry fluorescence intensity, confirming efficient activity of both sponges and synthetic *miR124*.

503UNC:Gal4 (variegated expression of Gal4 in muscle cells) and UAS:YFP-*miR124* in the βactin:mCherry-SP124 transgenic line (SP124). We targeted muscle cells as they do not express endogenous *miR-124*. Muscle cells expressing YFP-*miR124* appear as darkened regions on the ubiquitous mCherry-SP124 background, as *miR-124* binding to mCherry-SP124 mRNA inhibited mCherry translation [Fig. 1(D)].

A rescue model was obtained by crossing the above lines (*mpeg1*:Gal4; UAS:YFP-*dre-miR-124-1* and βactin:mCherry-SP124) with the end result being an *mpeg1* specific overexpression of *miR-124* on a ubiquitous *miR-124* loss-of-function background.

Control fish for microglia baseline measurements were from the *mpeg1*:mCherry-CAAX transgenic line. The microglia of the optic tectum were targeted for analysis (Fig. 2).

miR-124 Overexpression Induces Early Low Motility in Developing Microglia

Time-lapse sequences were taken for each of the four transgenic lines: control (*mpeg1*:mCherry-CAAX), *miR-124* overexpression (*mpeg1*:Gal4, UAS:YFP-*dre-miR-124-1*), *miR-124* sponge (βactin:mCherry-SP124, *mpeg1*:eGFP), and rescue (*mpeg1*:Gal4, UAS:YFP-*dre-mir-124-1*, βactin:mCherry-SP124). Each larva was imaged for 3 hours at time steps of 7.5 minutes and motility was measured as distance (μm) travelled over the time lapse period.

During normal development, primitive macrophage invasion of the CNS commences at ~35 hpf (Herbomel et al., 2001), and we have shown that transition to a low motility (lM) profile occurs at ~120 hpf (5dpf) (Svahn et al., 2013). This was replicated for the *mpeg1*:mCherry-CAAX control in this study [Fig. 3(A)]. A Kruskal-Wallis ANOVA indicated a significant difference between samples ($H = 75.34$, df = 4, $p = 1.7 \times 10^{-15}$) and bootstrap resampling indicated that the 3-4dpf and 5-7dpf periods were significantly different from one another but not different within periods. The motility dynamics of early microglia from our previous work were recapitulated in this study.

miR-124 overexpressing microglia showed a precocious low-motility phenotype from 3 and 4dpf [Fig. 3(B)], which was significantly lower than control (3dpf, $p = 1.04 \times 10^{-4}$; 4dpf, $p = 1.08 \times 10^{-13}$). Motility at 5, 6 and 7dpf remained low and stable, not significantly different from control (5dpf, $p = 0.22$; 6dpf, $p = 0.67$; 7dpf, $p = 0.94$). From these results, it appears that primitive macrophages expressing excess *miR-124* are induced to transition to the lM profile rapidly after entry into the CNS, from at least 72 hpf.

miR-124 Knockdown Induces Elevated Microglial Motility and Restores the Motility Progression in a Rescue Model

With ubiquitous expression of the *miR-124* sponge, microglia motility increased and showed greater fluctuation over the imaging period [Fig. 3(C), Supporting Information video 1]. At 3dpf motility was significantly higher than control ($p = 3.4 \times 10^{-11}$). At 4dpf motility was equal to control ($p = 0.23$). At 5dpf the step down did occur but was smaller in magnitude and motility remained significantly higher than control at 5 and 6dpf (5dpf, $p = 0.04$; 6dpf, $p = 1.3 \times 10^{-4}$). At 7dpf the motility was not significantly different from control (p=0.24). Thus, although knockdown of *miR-124* resulted in elevated motility and a delay to the lM profile in microglia, it did not keep the cells in this state permanently.

In the rescue, *miR-124* was overexpressed in microglia in the presence of the *miR-124* sponge. The motility profile was restored and the stepdown at 5dpf reinstated [Fig. 3(D)]. At 3 and 4dpf, motility of microglia in the rescue was significantly lower than *miR-124* sponge alone ($p = 4.05 \times 10^{-18}$, $p = 0.02$) and significantly higher than *miR-124* overexpression alone ($p = 9 \times 10^{-3}$, $p = 1.8 \times 10^{-7}$) [Fig. 3(E)]. At 3dpf microglia motility in the rescue was skewed lower than control and was significantly different at 3dpf but not 4dpf ($p = 0.03$, $p = 0.12$). The step down was recovered at 5dpf and motility was not significantly different from control at 5, 6 and 7dpf, (5dpf, $p = 0.77$; 6dpf, $p = 0.1$; 7dpf, $p = 0.16$).

In contrast to *miR-124* overexpression, a *miR-124* sponge delayed the transition to a lM profile. Given the specificity of the sponge to *miR-124*, the reinstatement of a normal development profile when both constructs were expressed in opposition indicates that the early lM profile induced by *miR-124* overexpression is likely to be an outcome of *miR-124* activity.

To determine if the effect on motility was accompanied by an alteration in process formation and retraction, we conducted an analysis of the stability of processes in which we recorded for each cell the maximum duration processes existed during the imaging period. In our previous study this metric increased during development, just as the time increased that microglia spent in the ramified morphology. In this analysis it was found that miR-124 modulation had no significant effect on this process (data not shown).
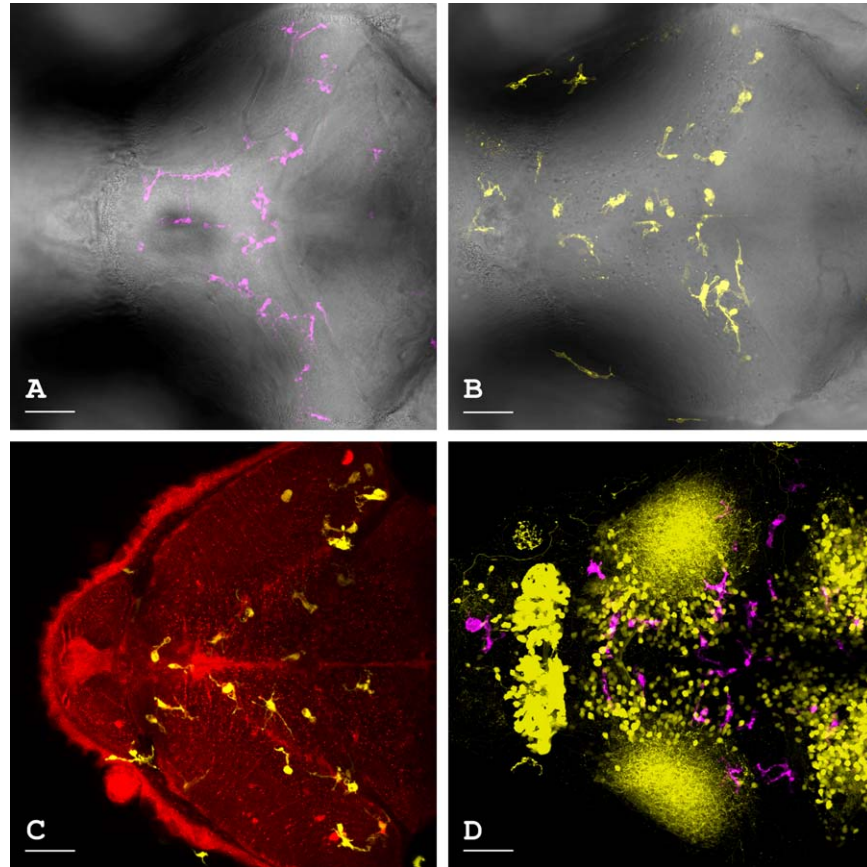
Figure 2 Examples of transgene expression. A: *mpeg1*:mCherry-CAAX that induced mCherry expression in microglia of the optic tectum. B: *mpeg1*:Gal4, UAS:YFP-*dre-miR-124-1* in microglia of the optic tectum. C: *mpeg1*:Gal4, UAS:YFP-*dre-miR-124-1* (*miR-124* expression in microglia) on a ubiquitous mCherry and *miR-124* sponge expression background. Note, *β*actin:mCherry-SP124, *mpeg1*:eGFP (*miR-124* sponge) is identical to this expression with eGFP in place of the YFP-*dre-miR-124-1*. D: *mpeg1*:mCherry-CAAX expressing mCherry in microglia of the optic tectum with *elavl3* driven YFP-*dre-miR-124-1*. No clear morphology differences were observed between the transgenic models. Subparts (A) and (B) are maximum intensity projections of the fluorophore channel overlaid on a single slice in the bright field channel at 5 and 6dpf, (C) is a maximum intensity projection of the YFP channel (representing the microglial *dre-miR-124-1* and YFP expression) overlaid on a single slice from the mCherry channel (representing *β*actin driven mCherry and sponge expression) at 5dpf, and (D) is a maximum intensity projection of the microglial mCherry expression and the *elavl3* driven *dre-miR-124-1* and YFP expression at 6dpf. Scale = 50μm.

Microglial *miR-124* Overexpression Induces Apoptotic Cell Build-Up

Previous analysis of microglial developmental progression in the optic tectum showed a prominent apoptotic cell clearance behavior. It was rare to observe an apoptotic cell that was not already in the process of being phagocytosed (Peri and Nüsslein-Volhard, 2008; Svahn et al., 2013) [Fig. 4(A)]. In the current study, examination of brightfield images revealed that the optic tectum in the majority of *miR-124* overexpressing larvae contained large numbers of apoptotic cells that had not entered the microglial phagocytic pathway [Fig. 4(B), a full stack of the tectum is shown in Supporting Information Fig. 2]. Apo-

ptotic cells were counted in a $50 \times 50 \times 50 \ \mu m^3$ cube of each tectal hemisphere. The control larvae in this study replicated the previous observation of low numbers of uncontacted apoptotic cells (mean = 1.19, CI: 0.59–1.8) with 34 of 46 hemispheres having a count of 0 or 1. Similarly, ubiquitous *miR-124* sponge expression showed a low number of uncontacted apoptotic cells (mean = 0.65, CI: 0.33–0.97) with 36 of 40 hemispheres recording a count of 0 or 1. The number of uncontacted apoptotic cells was high for both *miR-124* overexpression (mean = 18.06, CI: 12.8–23.32) and the rescue (mean = 8.76, CI: 5.97–11.55). The difference between the *miR-124* overexpression and the rescue was significant ($p = 0.02$). As the phenotype was 60% penetrant in this study, we analyzed

separately larvae in which the number of uncontacted apoptotic cells in at least one hemisphere was ≥ 10. Within these specimens, the phenotype in *miR-124* overexpression alone was significantly more severe than when *miR-124* overexpression was opposed by
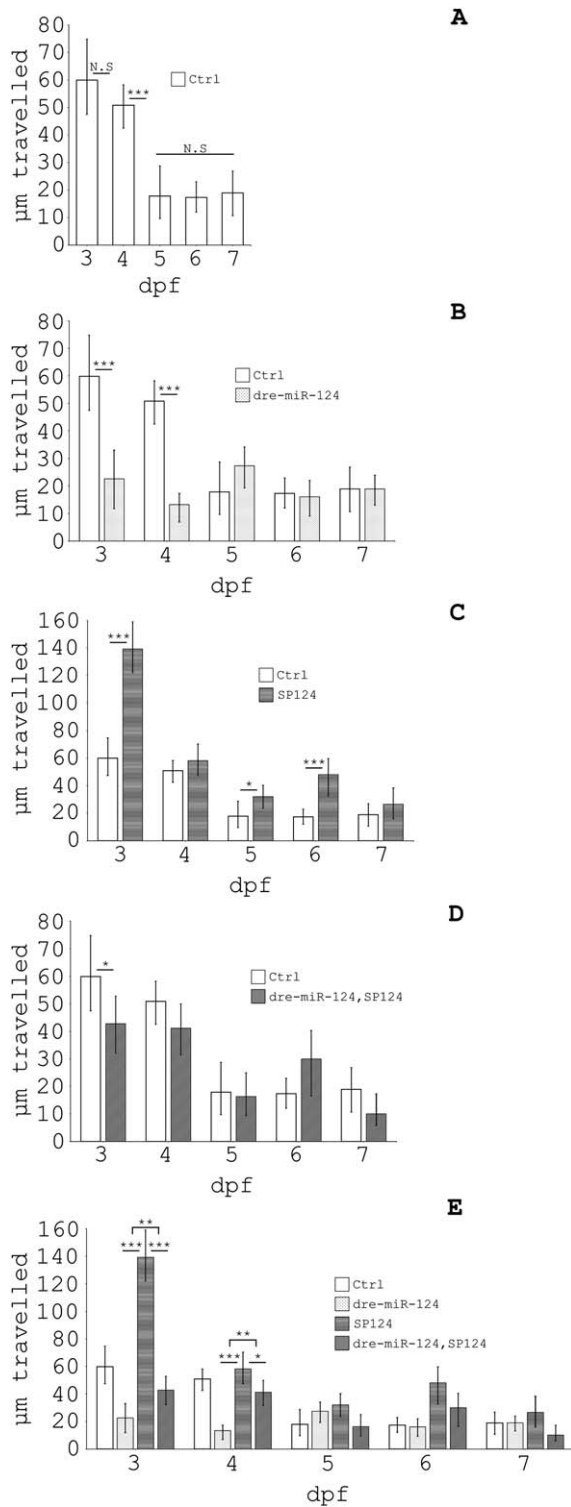
the *miR-124* sponge [Fig. 4(C)] (CIs: *miR-124* overexpression, 38-70; rescue, 26–39; $p = 0.015$).

miR-124 is an important miRNA for neuronal development (Makeyev et al., 2007). In addition, miRNAs bound in exosomes may be secreted into the extracellular space and transferred between cells (Valadi et al., 2007; Lachenal et al., 2011; Chen et al., 2012). To determine whether excess *miR-124* in neurons alone was sufficient to induce the phenotype, we carried out imaging with *elavl3*:Gal4; UAS:YFP-*dre-miR-124-1*; *mpeg1*:mCherry-CAAX larvae. In these larvae the number of apoptotic cells did not differ from control (mean=1.5, CI: 0.05–2.94) with 14 of 18 hemispheres showing 0 or 1 uncontacted apoptotic cells.

In summary, a phenotype of apoptotic cell build-up occurred in the majority of larvae overexpressing *miR-124*. Of note, over the imaging period no correlation between age and uncontacted apoptotic cell number was observed. This may indicate that an equilibrium point between apoptosis and

Figure 3 Motility of microglia, measured as distance moved in 3 hours, in the optic tectum during the 3 to 7dpf period. A: *mpeg1*:mCherry-CAAX motility. Control microglia had a median motility of 59.89 μm and 50.82 μm on 3 and 4dpf (CIs: 47.44–74.76 μm; 42.5–58.18 μm). Median motility was 17.87μm, 17.34μm and 18.91μm at 5, 6 and 7dpf (CIs: 9.69-28.71μm; 12–22.94 μm; 10.68–26.83 μm). Significant differences were found between the 3–4 and 5–7dpf periods, but not within the periods (3–5 dpf, $p = 8 \times 10^{-7}$; 3–6 dpf, $p = 8.4 \times 10^{-9}$; 3–7 dpf, $p = 2.6 \times 10^{-7}$; 4–5 dpf, $p = 8 \times 10^{-7}$; 4–6 dpf, $p = 1.5 \times 10^{-6}$; 4–7 dpf, $p = 3 \times 10^{-8}$; 3–4 dpf, $p = 0.18$; 5–6 dpf, $p = 0.76$; 5–7 dpf, $p = 0.96$; 6–7 dpf, $p = 0.81$). B: *mpeg1*:Gal4, UAS:YFP-*dre-miR-124*−1 motility. *mir-124* overexpressing microglia had a median motility of 22.56 μm and 13.25 μm at 3 and 4 dpf respectively (CIs: 11.84–33 μm; 6.91–17.29 μm) and 27.34 μm, 16.07 μm, and 18.94 μm at 5, 6 and 7 dpf, respectively (CIs: 19.3–34.12 μm; 3.09–22.03 μm; 13.01–23.91 μm). C: *β*actin:mCherry-SP124, *mpeg1*:eGFP motility. Microglia on the *miR-124* sponge background had median motility of 139.27 μm and 58.16 μm at 3 and 4 dpf, respectively (CIs: 122.16–158.9 μm; 47.28–70.32 μm) and 32.11 μm, 48.11 μm, and 26.57 μm at 5, 6, and 7 dpf, respectively (CIs: 23.79–40.21 μm; 32.73–59.59 μm; 15.8–38.3 μm). D: Rescue (*mpeg1*:Gal4, UAS:YFP-*dre-miR-124-1*; *β*actin:mCherry-SP124) motility. Microglia motility in the rescue was 42.72 μm and 41.1 μm at 3 and 4 dpf, respectively, (CIs: 32.17–52.75 μm; 31.43–49.93 μm) and 16.32 μm, 29.96 μm, and 10.05 μm at 5, 6 and 7 dpf respectively (CIs: 9.5–24.94 μm; 16.57–40.33 μm; 5.84–17.28 μm). Kruskal-Wallis ANOVA supported a significant difference between days ($H = 48.04$, df = 4, $p = 9.26 \times 10^{-10}$). E: Combined motility results.
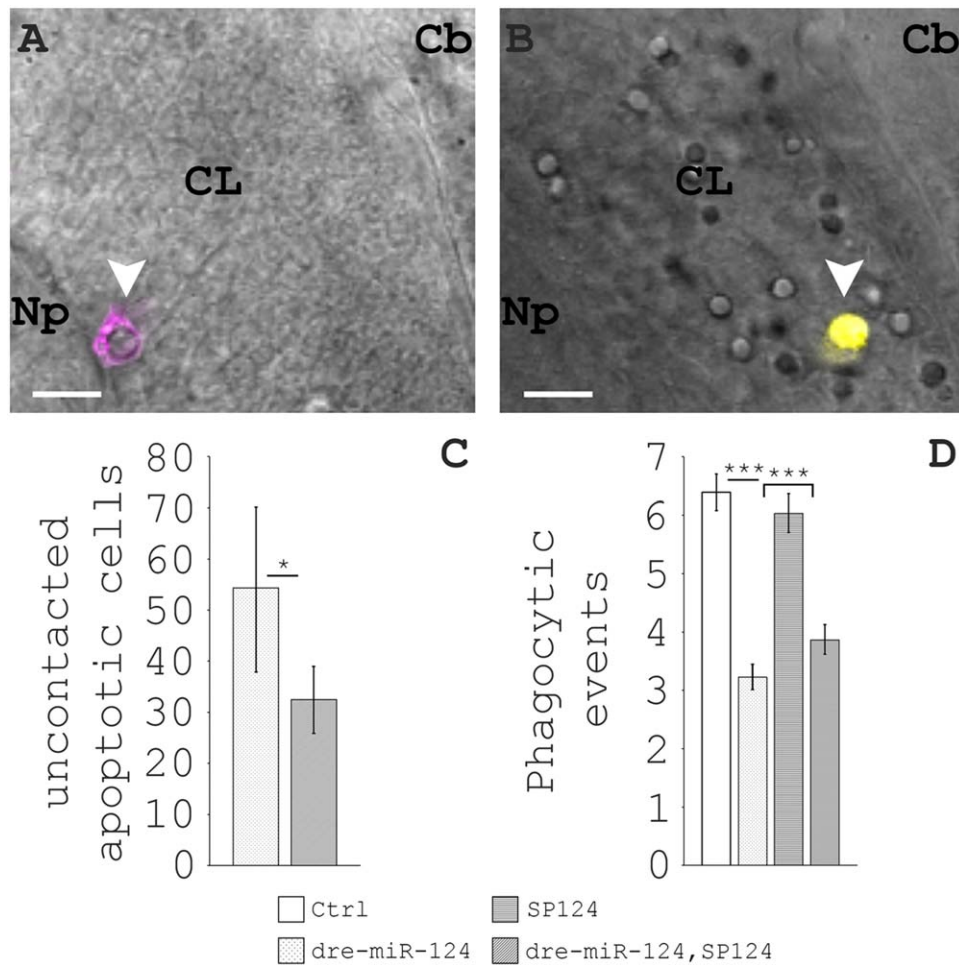
Figure 4 Successful microglial scavenging versus left over apoptotic cells. A: Representative region of the optic tectum of an *mpeg1*:mCherry-CAAX larva at 5dpf. The arrow indicates an apoptotic cell which stands out from the cell layer background, the magenta coloured signal is a microglial process engulfing the cell. B: A representative region of the optic tectum of an *mpeg1*:Gal4, UAS:YFP-*dre-miR-124-1* larvae at 5dpf. Many free-lying apoptotic cells are present on top of the cell layer, the yellow signal is a microglial process in contact with a dead cell. CB, cerebellum, CL, cell layer, Np, neuropil. Scale = 10 μm. C: Residual apoptotic cell body counts for the *miR-124* overexpression and rescue in larvae when $\geq$10 occurred in one or both tectal hemispheres. D: Phagocytic profile of microglia in the optic tectum over the 3-7dpf period. Control microglia, CI: 6.08–6.7; *miR-124* overexpressing, CI: 3.01–3.45; *miR-124* sponge, CI: 5.7–6.37; rescue, CI: 3.62-4.13.

phagocytosis may exist as higher numbers of apoptotic cells could be caused by increased induction of apoptosis or reduced clearance of apoptotic cells; however either of these would be expected to cause a gradually worsening phenotype.

miR-124 Reduces the Clearance Rate of Apoptotic Cells by Microglia During Development

In our previous analysis the number of cells phagocytosed over the imaging period remained constant over the 3–9dpf period. This was replicated for control larvae in the current study at 6.39 cells/3hrs and one-way ANOVA indicated no significant difference between days ($F(4,149)=1.41$, $p = 0.23$) [Fig. 4(D)]. *miR-124* overexpression significantly reduced the clearance rate of apoptotic cells to 3.23 ($p < 1 \times 10^{-10}$). The *miR-124* sponge alone did not induce a significant change in the phagocytic profile ($p = 0.12$). The rescue induced a partial recovery to 3.87, which was higher than the *miR-124* overexpression ($p = 2 \times 10^{-4}$) and lower than the control ($p = 3.6 \times 10^{-5}$).

Taken together, it appears that the presence of elevated levels of *miRNA-124* in microglia resulted in a

low phagocytosis (lP) profile which reduces the clearance capacity of microglia during development.

Survival and Microglia Development Controls Indicate *miR-124* Activity is Specific

Overexpression of any miRNA may result in a generalized nonspecific miRNA depletion, as the overabundant pri/pre-miRNA monopolises the miRNA processing machinery. A proxy for this phenomenon can be found in *dicer*^{-/-} zebrafish mutants, wherein processing of all pre-miRNAs to mature miRNAs is abolished. A maternal zygotic *dicer*^{-/-} mutant (Giraldez et al., 2005) displayed a failure of the programs for formation of the neural tube from the neural rod and for formation of the ventricles and the folding of the neural tissue into distinct boundaries. Central nervous system axis formation was preserved, while the morphological program was severely disrupted. A number of axonal projections were noted to be misrouted and misplaced sensory neurons were observed, indicating that cell specification and patterning of neuronal networks was also disrupted. A simple and well characterized touch-response reflex (Pietri et al., 2009) was significantly attenuated. For the *miR-124* overexpression and the *miR-124* sponge a 2-week survival and touch response period was carried out. The *miR-124* overexpression and *miR-124* sponge larvae developed without any morphological abnormalities above background level ($n = 50$ for each transgene and each control) and touch response was normal for both transgenes.

As a control for a general miRNA depletion underlying the motility, apoptosis and phagocytosis results of this study; *miR-218* was overexpressed in place of *miR-124*. *miR-218* is predominantly expressed in motor neurons (Punnamoottil et al., 2015) and is not currently known to bind any prominent targets expressed in microglia. *mpeg1*:Gal4, UAS:YFP-*hsa-miR-218-2* larvae did not differ from control in motility (CIs: 3dpf, 45–58.46 μm, $p = 0.29$; 4dpf, 44.93–58.49, $p = 0.82$; 5dpf, 8.56–34.73, $p = 0.78$; 6dpf, 12.03–21.43, $p = 0.85$), uncontacted apoptotic cells (mean=1.1, CI: 0.72–1.48) or phagocytic profile (CI: 4.43–6.34, $p = 0.2$) (analysis conducted for 3-6dpf as 7dpf data was not available).

In conclusion, we show here that overexpression of *miR-124* specifically in microglia, but not in neurons, results in a lM and a lP profile of developing microglia, strongly suggesting that *miR-124* has a role during the developmental transition of early amoeboid microglia to mature sessile microglia.

DISCUSSION

Macrophage (*mpeg1*) targeted *miR-124* overexpression induced an early low motility (lM) and low phagocytosis (lP) profile in microglia resulting in a reduced clearance rate of apoptotic cells and an increase in the number of apoptotic cell bodies in the developing optic tectum. Conversely, a sponge-mediated knockdown of *miR-124* increased the motility of the microglia and partially rescued the lM and lP profiles when coexpressed in *miR-124* overexpressing animals. Importantly, overexpression of *miR-124* in postmitotic neurons alone was not sufficient to induce accumulation of residual apoptotic cells, and overexpression of an unrelated miRNA (*miR-218*) in microglia did not result in their deviation from the normal microglial developmental profile, indicating that *miR-124* modulation specifically in microglia was driving the abnormal developmental trajectory.

Ponomarev et al. (2011) conducted RT-PCR profiling to characterize the miRNA profile of macrophages in different organ niches. After sorting of Cd11b^{+}, F4/80[+] macrophages from a subset of tissue specific phagocyte populations of the mouse, *miR-124* was identified in microglia of the CNS. In contrast, *miR-223* was identified in peripheral macrophages only; indicating that tissue-specific macrophage populations may exhibit distinct miRNA profiles.

miR-124 was shown to exert an influence on microglial and macrophage marker expression by means of downregulation of C/EBP-α via three conserved 7-mer binding sites in the *CEBPA* mRNA (Ponomarev et al., 2011). We found that the zebrafish *cebpa* 3'UTR contains two predicted *miR-124* binding sites (TargetScan 6.2, Grimson et al., 2007). C/EBP-α is a well-characterized master transcription factor in myeloid cells (Iwama et al., 1998; Yeamans et al., 2007) and in microglia, C/EBP-α is associated with the response to pathological challenges and development into the full-blown adult macrophage phenotype (Walton et al., 1998; Nishiyama et al., 2004; Yeamans et al., 2007; Bristol et al., 2009). One of the major targets of CEBP-α is PU.1 (encoded by *SPI1*/spi1), which is repressed as a consequence of *miR-124* mediated CEBP-α downregulation. PU.1 is a master regulator of macrophage and microglia fate determination (Kierdorf et al., 2013), which is associated with the majority of macrophage lineage enhancer regions (Ghisletti et al., 2010). It is therefore reasonable to assume that a reduction of PU.1 may lead to a weakened induction of genes subserving a wide range of microglial response pathways, essentially dulling the senses of the microglia. However, the output of any

given microglial pathway under PU.1 suppression would have to be assessed on a contextual basis (Svahn et al., 2014) (e.g. development, senescence, glioma).

Recently *miR-124* was found to be downregulated in neurons in a mouse model of frontotemporal dementia (Gascon et al., 2014). In this case, the effect of *miR-124* downregulation was overexpression of the AMPA receptor mRNAs of *GRIA2*, *GRIA3* and *GRIA4*. Using TargetScan we found conserved *miR-124* binding sites in the 3'UTRs of zebrafish *gria2a/b*, *gria3a* and *gria4a/b* (Hoppmann et al., 2008). However, from the results of the current study, it is unlikely that overexpression of AMPA receptors influenced microglial motility as neither overexpression of *miR-124* in neurons using the *elavl3* promoter, nor expression of *mir-218*, which also has conserved binding sites in *gria2a/b* and *gria4b*, had any detectable effect.

Phagocytosis requires sensing, migration, cytoskeletal rearrangement and lysis. Using TargetScan we could find no conserved binding sites for *miR-124* in a panel of microglial receptor mRNAs associated with phagocytosis (selected from Kettenmann et al., 2011), including the Fc receptors identified in microglia (Linnartz and Neumann, 2012), the purinergic receptors $P2X_{1-7}$, $P2Y_{1,2,4,6,12}$ (Xiang and Burnstock, 2005; Bennett et al., 2008), *TREM1/2* and *Dap12* (*TYROBP*) (Wakselman et al., 2008). Impaired lysis would be expected to result in enlarged, rounded and highly vacuolated cell bodies as phagocytic vesicles accumulate. This was not observed in the microglia in this study, suggesting a failure of lysis was not the cause of impaired clearance.

Cytoskeletal rearrangement is vital to successful phagocytosis. A component of phagocytosis in macrophages, *ELMO2* (*elmo2*) (Gumienny et al., 2001; Margaron et al., 2013), was predicted to contain a binding site for *mir-124* conserved between humans and zebrafish. ELMO1 and ELMO2 are the vertebrate homologs (88% similarity between homologues) of the *ced-12* gene, initially identified as part of the cell migration and engulfment pathway in C.*elegans* (Gumienny et al., 2001). The ELMO protein interacts with the DOCK180 protein in a Rac activating pathway and enables cytoskeletal rearrangement. In a zebrafish *elmo1*^{-/-} mutant, developing microglia migrated toward apoptotic cells but were frequently unable to initiate successful phagocytosis (van Ham et al., 2012).

In addition, a cytoskeletal component, vimentin (*vim*), was predicted to contain two conserved targets for *miR-124*. In mammals, vimentin is upregulated as adult microglia become activated in response to pathological challenges (Graeber et al., 1988). The time course of reactive vimentin protein expression in microglia activated by peripheral nerve axotomy led to the hypothesis that it may have a role in the rapid,

highly plastic morphological changes that characterize dividing, migrating and phagocytic motile microglia. In microglia cell culture, increased availability of fibronectin induces a significant reduction in vimentin phosphorylation and in turn vimentin disassembly (Chamak and Mallat, 1991) coinciding with transition of the microglia into ramified cells. Based on the observations of this study and the predicted, conserved targets of *miR-124* above, we suggest that by post-transcriptionally inhibiting vimentin or ELMO2, *miR-124* may positively regulate the lM, lP microglial developmental profile without blocking the capacity of microglia to become motile, phagocytic cells.

Taken together, we conclude that the mechanisms by which tissue macrophages acquire regionalized phenotypes are likely to include miRNAs. Specifically, we have shown that *miR-124* downregulates cellular motility and phagocytic capacity in developing microglia, features that are essential for the generation of the ramified microglia of the adult CNS.

REFERENCES

Åkerblom M, Sachdeva R, Barde I, Verp S, Gentner B, Trono D, Jakobsson J. 2012. MicroRNA-124 is a subventricular zone neuronal fate determinant. J Neurosci 32: 8879–8889.

Altman DG, Bland JM. 2011. How to obtain the P value from a confidence interval. BMJ 343:d2304

Bartel DP. 2009. MicroRNAs: Target recognition and regulatory functions. Cell 136:215–233.

Bennett MR, Buljan V, Farnell L, Gibson WG. 2008. Purinergic junctional transmission and propagation of calcium waves in cultured spinal cord microglial networks. Purinergic Signal 4:47–59.

Bristol JA, Morrison TE, Kenney SC. 2009. CCAAT/enhancer binding proteins α and β regulate the tumor necrosis factor receptor 1 gene promoter. Mol Immunol 46:2706–2713.

Cao X, Pfaff SL, Gage FH. 2007. A functional study of miR-124 in the developing neural tube. Genes Dev 21:531–536.

Chamak B, Mallat M. 1991. Fibronectin and laminin regulate the in vitro differentiation of microglial cells. Neuroscience 45:513–527.

Chen C, Li H, Liu Y, Guo Z, Wu H, Li X, Lou H, et al. 2015. A novel size-based sorting mechanism of pinocytic luminal cargoes in microglia. J Neurosci 35:2674–2688.

Chen X, Liang H, Zhang J, Zen K, Zhang C-Y. 2012. Secreted microRNAs: A new form of intercellular communication. Trends Cell Biol 22:125–132.

Ebert MS, Neilson JR, Sharp PA. 2007. MicroRNA sponges: Competitive inhibitors of small RNAs in mammalian cells. Nat Methods 4:721–726.

Ebert MS, Sharp PA. 2010. MicroRNA sponges: Progress and possibilities. RNA 16:2043–2050.

Ellett F, Pase L, Hayman JW, Andrianopoulos A, Lieschke GJ. 2011. mpeg1 promoter transgenes direct macrophage-lineage expression in zebrafish. Blood 117:e49–e56.

Friedman RC, Farh KK-H, Burge CB, Bartel DP. 2009. Most mammalian mRNAs are conserved targets of micro-RNAs. Genome Res 19:92–105.

Gascon E, Lynch K, Ruan H, Almeida S, Verheyden JM, Seeley WW, Dickson DW, et al. 2014. Alterations in microRNA-124 and AMPA receptors contribute to social behavioral deficits in frontotemporal dementia. Nat Med 20:1444–1451.

Ghisletti S, Barozzi I, Mietton F, Polletti S, De Santa F, Venturini E, Gregory L, et al. 2010. Identification and characterization of enhancers controlling the inflammatory gene expression program in macrophages. Immunity 32:317–328.

Ginhoux F, Greter M, Leboeuf M, Nandi S, See P, Gokhan S, Mehler MF, et al. 2010. Fate mapping analysis reveals that adult microglia derive from primitive macrophages. Science 330:841–845.

Giraldez AJ, Cinalli RM, Glasner ME, Enright AJ, Thomson JM, Baskerville S, Hammond SM, et al. 2005. MicroRNAs regulate brain morphogenesis in zebrafish. Science 308:833–838.

Graeber MB. 2010. Changing face of microglia. Science 330:783–788.

Graeber MB, Streit WJ, Kreutzberg GW. 1988. The microglial cytoskeleton: Vimentin is localized within activated cells in situ. J Neurocytol 17:573–580.

Grimson A, Farh KK-H, Johnston WK, Garrett-Engele P, Lim LP, Bartel DP. 2007. MicroRNA targeting specificity in mammals: Determinants beyond seed pairing. Mol Cell 27:91–105.

Gumienny TL, Brugnera E, Tosello-Trampont AC, Kinchen JM, Haney LB, Nishiwaki K, Walk SF, et al. 2001. CED-12/ELMO, a novel member of the CrkII/Dock180/Rac pathway, is required for phagocytosis and cell migration. Cell 107:27–41.

Herbomel P, Thisse B, Thisse C. 2001. Zebrafish early macrophages colonize cephalic mesenchyme and developing brain, retina, and epidermis through a M-CSF receptor-dependent invasive process. Dev Biol 238:274–288.

Hoeffel G, Chen J, Lavin Y, Low D, Almeida FF, See P, Beaudin AE, et al. 2015. C-Myb+ erythro-myeloid progenitor-derived fetal monocytes give rise to adult tissue-resident macrophages. Immunity 42:665–678.

Hoppmann V, Wu JJ, Søviknes AM, Helvik JV, Becker TS. 2008. Expression of the eight AMPA receptor subunit genes in the developing central nervous system and sensory organs of zebrafish. Dev Dyn 237:788–799.

Isik M, Korswagen HC, Berezikov E. 2010. Expression patterns of intronic microRNAs in Caenorhabditis elegans. Silence 1:5.

Iwama A, Zhang P, Darlington GJ, McKercher SR, Maki R, Tenen DG. 1998. Use of RDA analysis of knockout mice to identify myeloid genes regulated in vivo by PU.1 and C/EBPα. Nucleic Acids Res 26:3034–3043.

Kettenmann H, Hanisch UK, Noda M, Verkhratsky A. 2011. Physiology of microglia. Physiol Rev 91:461–553.

Kierdorf K, Erny D, Goldmann T, Sander V, Schulz C, Perdiguero EG, Wieghofer P, et al. 2013. Microglia emerge from erythromyeloid precursors via Pu.1- and Irf8-dependent pathways. Nat Neurosci 16:273–280.

Lachenal G, Pernet-Gallay K, Chivet M, Hemming FJ, Belly A, Bodon G, Blot B, et al. 2011. Release of exosomes from differentiated neurons and its regulation by synaptic glutamatergic activity. Mol Cell Neurosci 46: 409–418.

Lagos-Quintana M, Rauhut R, Yalcin A, Meyer J, Lendeckel W, Tuschl T. 2002. Identification of tissue-specific micrornas from mouse. Curr Biol 12:735–739.

Lim LP, Glasner ME, Yekta S, Burge CB, Bartel DP. 2003. Vertebrate microrna genes. Science 299:1540.

Linnartz B, Neumann H. 2012. Microglial activatory (immunoreceptor tyrosine-based activation motif)- and inhibitory (immunoreceptor tyrosine-based inhibition motif)-signaling receptors for recognition of the neuronal glycocalyx. Glia 61:37–46.

Makeyev EV, Zhang J, Carrasco MA, Maniatis T. 2007. The microRNA miR-124 promotes neuronal differentiation by triggering brain-specific alternative pre-mRNA splicing. Mol Cell 27:435–448.

Margaron Y, Fradet N, Côté JF. 2013. ELMO recruits actin cross-linking family 7 (ACF7) at the cell membrane for microtubule capture and stabilization of cellular protrusions. J Biol Chem 288:1184–1199.

Nishiyama C, Nishiyama M, Ito T, Masaki S, Masuoka N, Yamane H, Kitamura T, et al. 2004. Functional analysis of PU.1 domains in monocyte-specific gene regulation. FEBS Lett 561:63–68.

Otaegi G, Pollock A, Sun T. 2012. An optimized sponge for microRNA miR-9 affects spinal motor neuron development in vivo. Front Neurosci 5:146.

Paquet D, Bhat R, Sydow A, Mandelkow E, Berg S, Hellberg S, Fälting J, et al. 2009. A zebrafish model of tauopathy allows in vivo imaging of neuronal cell death and drug evaluation. J Clin Invest 119:1382–1395.

Peri F, Nüsslein-Volhard C. 2008. Live imaging of neuronal degradation by microglia reveals a role for v0-ATPase a1 in phagosomal fusion in vivo. Cell 133: 916–927.

Pietri T, Manalo E, Ryan J, Saint-Amant L, Washbourne P. 2009. Glutamate drives the touch response through a rostral loop in the spinal cord of zebrafish embryos. Dev Neurobiol 69:780–795.

Ponomarev ED, Veremeyko T, Barteneva N, Krichevsky AM, Weiner HL. 2011. MicroRNA-124 promotes microglia quiescence and suppresses EAE by deactivating macrophages via the C/EBP-α-PU.1 pathway. Nat Med 17:64–70.

Punnamoottil B, Rinkwitz S, Giacomotto J, Svahn AJ, Becker TS. 2015. Motor neuron-expressed microRNAs 218 and their enhancers are nested within introns of SLIT2/3 genes. Genesis 53:321–328.

Sanuki R, Onishi A, Koike C, Muramatsu R, Watanabe S, Muranishi Y, Irie S, et al. 2011. miR-124a is required for

hippocampal axogenesis and retinal cone survival through Lhx2 suppression. Nat Neurosci 14:1125–1134.

Scott EK. 2009. The Gal4/UAS toolbox in zebrafish: New approaches for defining behavioral circuits. J Neurochem 110:441–456.

Svahn AJ, Becker TS, Graeber MB. 2014. Emergent properties of microglia. Brain Pathol 24:665–670.

Svahn AJ, Graeber MB, Ellett F, Lieschke GJ, Rinkwitz S, Bennett MR, Becker TS. 2013. Development of ramified microglia from early macrophages in the zebrafish optic tectum. Dev Neurobiol 73:60–71.

Valadi H, Ekström K, Bossios A, Sjöstrand M, Lee JJ, Lötvall JO. 2007. Exosome-mediated transfer of mRNAs and microRNAs is a novel mechanism of genetic exchange between cells. Nat Cell Biol 9:654–659.

Van Ham TJ, Kokel D, Peterson RT. 2012. Apoptotic cells are cleared by directional migration and elmo1- dependent macrophage engulfment. Curr Biol 22:830–836.

Visvanathan J, Lee S, Lee B, Lee JW, Lee S. 2007. The microRNA miR-124 antagonizes the anti-neural REST/ SCP1 pathway during embryonic CNS development. Genes Dev 21:744–749.

Wakselman S, Béchade C, Roumier A, Bernard D, Triller A, Bessis A. 2008. Developmental neuronal death in hippocampus requires the microglial CD11b integrin and DAP12 immunoreceptor. J Neurosci 28:8138–8143.

Walton M, Saura J, Young D, MacGibbon G, Hansen W, Lawlor P, Sirimanne E, et al. 1998. CCAAT-enhancer binding proteinα is expressed in activated microglial cells after brain injury. Mol Brain Res 61:11–22.

Westerfield M. 2000. The Zebrafish Book: A Guide for the Laboratory Use of Zebrafish (Danio rerio). Eugene, OR: University of Oregon Press.

Xiang Z, Burnstock G. 2005. Expression of P2X receptors on rat microglial cells during early development. Glia 52: 119–126.

Yeamans C, Wang D, Paz-Priel I, Torbett BE, Tenen DG, Friedman AD. 2007. C/EBPα binds and activates the PU. 1 distal enhancer to induce monocyte lineage commitment. Blood 110:3136–3142.

Yu JY, Chung KH, Deo M, Thompson RC, Turner DL. 2008. MicroRNA miR-124 regulates neurite outgrowth during neuronal differentiation. Exp Cell Res 314:2618–2633.